

Comparison of QuickBird satellite imagery and airborne imagery for mapping grain sorghum yield patterns

Chenghai Yang · James H. Everitt · Joe M. Bradford

© Springer Science + Business Media, Inc. 2006

Abstract Timely and accurate information on crop conditions obtained during the growing season is of vital importance for crop management. High spatial resolution satellite imagery has the potential for mapping crop growth variability and identifying problem areas within fields. The objectives of this study were to use QuickBird satellite imagery for mapping plant growth and yield patterns within grain sorghum fields as compared with airborne multispectral image data. A QuickBird 2.8-m four-band image covering a cropping area in south Texas, USA was acquired in the 2003 growing season. Airborne three-band imagery with submeter resolution was also collected from two grain sorghum fields within the satellite scene. Yield monitor data collected from the two fields were resampled to match the resolutions of the airborne imagery and the satellite imagery. The airborne imagery was related to yield at original submeter, 2.8 and 8.4 m resolutions and the QuickBird imagery was related to yield at 2.8 and 8.4 m resolutions. The extracted QuickBird images for the two fields were then classified into multiple zones using unsupervised classification and mean yields among the zones were compared. Results showed that grain yield was significantly related to both types of image data and that the QuickBird imagery had similar correlations with grain yield as compared with the airborne imagery at the 2.8 and 8.4 m resolutions. Moreover, the unsupervised classification maps effectively differentiated grain production levels among the zones. These results indicate that high spatial resolution satellite imagery can be a useful data source for determining plant growth and yield patterns for within-field crop management.

Keywords Airborne imagery · Grain sorghum · High resolution · QuickBird imagery · Remote sensing · Yield monitor · Yield patterns

C. Yang (✉) · J. H. Everitt · J. M. Bradford
USDA-ARS Kika de la Garza Subtropical Agricultural Research Center,
2413 E. Highway 83, Weslaco, TX, 78596 USA
e-mail: cyang@weslaco.ars.usda.gov

Introduction

High resolution imagery from the Space Imaging IKONOS and DigitalGlobe QuickBird commercial satellites has been available for a few years. The commercial availability of high resolution satellite data has opened up new opportunities not only for applications that employ traditional satellite imagery such as Landsat but also for those that require high resolution remote sensing data. Precision agriculture is one of the applications that will benefit from the high resolution satellite sensors. Until the recent launches of these two satellite systems, satellite imagery had limited use for precision agriculture, mainly because of its coarse spatial resolution. Since precision farming requires detailed information about soil and crop conditions, a spatial resolution of a few meters is required and some specific applications such as weed detection and management may need resolutions in the order of centimeters (Robert 1996). Therefore, aerial photographic cameras and airborne video and digital imaging systems have been more widely used in both research and commercial operations for precision agriculture. Airborne imaging systems can provide multispectral image data at spatial resolutions ranging from less than 1 m to a few meters with up to 12 discrete narrow spectral bands in the visible to near-infrared (NIR) regions of the electromagnetic spectrum (Everitt et al. 1995; Mao and Kettler 1995; Escobar et al. 1997; Escobar et al. 1998). Airborne multispectral imagery has been used for assessing soil and plant growth variability, mapping crop yields, and detecting crop stress (Johannsen et al. 1998; Senay et al. 1998; Yang and Anderson 1999; Barnes and Baker 2000; Yang 2000; Yang and Everitt 2002; Pinter et al. 2003).

When Space Imaging successfully launched the IKONOS satellite in 1999, it made history with the world's first high resolution commercial remote sensing satellite for civilian uses. IKONOS records four channels of multispectral data at 4 m resolution and one panchromatic channel with 1 m resolution. Two years later, DigitalGlobe successfully deployed the QuickBird satellite, which provides four channels of multispectral data with 2.4 m (at nadir) or 2.8 m (off nadir) resolution and one panchromatic channel with 0.6 or 0.7 m resolution. These two satellite sensors have significantly narrowed the gap in spatial resolution between satellite and airborne imagery. In addition to their high spatial resolution, both sensors offer image data with an 11-bit dynamic range. The high radiometric resolution is much better than the 8-bit resolution from the traditional satellite sensors, such as Landsat TM, SPOT and many airborne imaging sensors.

Broad band vegetation indices, such as the ratio vegetation index (RVI) and the normalized difference vegetation index (NDVI), have been widely used to quantify crop variables such as yield, biomass, leaf area index and plant height (Tucker et al. 1980; Wiegand and Richardson 1990; Thenkabail et al. 1995). Airborne multispectral imagery has been used for estimating crop yield for precision agriculture in recent years due to its high spatial and spectral resolutions (Yang and Anderson 1999; Gopala Pillai and Tian 1999; Shanahan et al. 2001). Both spectral bands and vegetation indices, such as band ratios and NDVI, derived from airborne multispectral imagery, have been related to yield monitor data for mapping yield variability (Senay et al. 1998; Yang et al. 2000; Yang and Everitt 2002). As high resolution satellite imagery is becoming commercially available, it is necessary to evaluate this type of image data for assessing crop conditions as compared with airborne multispectral image data. The objectives of this study were to (1) examine QuickBird imagery for mapping grain sorghum growth and yield variability; and (2) relate yield monitor data with QuickBird image data and airborne image data and compare the two types of imagery for yield estimation.

Methods

The study site was located in an intensively cropped area in the Rio Grande Valley of south Texas, USA. The soils in the area include grayish brown fine sandy loam, dark brown fine sandy loam, dark gray sandy clay loam and dark gray clay loam. The surface layer is about 0.3–0.5 m thick. The subsoil extends to a depth of 1.6 m or more. The topography in this area is nearly level to gently sloping (1–3% slopes). Grain sorghum and cotton are the major crops grown in the area, though citrus, sugarcane, and other crops are also cultivated. Most fields in the area are flood irrigated. Grain sorghum is typically planted in late February and harvested in June and July. Two grain sorghum fields, referred to as fields 1 and 2, were selected for this study. The areas for fields 1 and 2 were 23 and 20 ha, respectively. The fields were planted in late February. The sorghum variety was AgriPro 9850 and the seeding rate was approximately 250,000 seeds/ha.

A QuickBird image covering approximately an 11.35 km by 5.65 km rectangular area (64 km²) was acquired on 15 May 2003 by DigitalGlobe Inc. (Longmont, Colorado, USA). The geographic coordinates at the center of the area are (98°00'15" W, 26°28'28" N). The imagery contained four spectral bands: blue (450–520 nm), green (520–600 nm), red (630–690 nm) and NIR (760–900 nm). The spatial resolution of the imagery was 2.8 m (off-nadir). Prior to delivery, the imagery was radiometrically and geometrically corrected and rectified to the world geodetic survey 1984 (WGS84) datum and the universal transverse Mercator (UTM) coordinate system. The pre-rectified standard imagery had an average absolute positional error of 23 m and a root mean square (RMS) error of 14 m. To improve the positional accuracy, the pre-rectified imagery was further rectified based on a set of ground control points collected from the imaging area with a submeter-accuracy global positioning system (GPS) Pathfinder Pro XRS receiver (Trimble Navigation Limited, Sunnyvale, California, USA). The RMS error of the re-rectified imagery was reduced to approximately 5 m. For radiometric calibration, reflectance spectra were taken 2 weeks after imagery acquisition from three sites (an asphalt road, a concrete parking lot, and a caliche pavement) within the satellite scene. These pseudo-invariant features represented a wide range of reflectance values and had stable reflectance response within the two-week period. The reflectance spectra for the three pseudo-invariant features were measured using a FieldSpec Handheld spectroradiometer (Analytical Spectral Devices, Inc., Boulder, Colorado, USA) sensitive in the 350 to 1050 nm portion of the spectrum with a nominal spectral resolution of 1.4 nm. The rectified QuickBird image was converted to reflectance based on four calibration equations (one for each band) relating reflectance values to the digital count values on the three features. All procedures for image rectification and calibration were performed using ERDAS IMAGINE (ERDAS, Inc., Atlanta, Georgia, USA).

Airborne color-infrared (CIR) digital imagery was acquired using a digital imaging system described by Escobar et al. (1997) from the two grain sorghum fields on 30 May 2003. The imaging system consisted of three Kodak MegaPlus digital charge coupled device (CCD) cameras. The acquisition computer and image grabbing cards were upgraded to enhance acquisition speed and obtain higher resolution imagery. The enhanced system had the capability of obtaining images with 1280 × 1024 pixels as compared with the 1024 × 1024 pixels the old system had. The cameras were sensitive in the visible to NIR regions (400–1000 nm) and had a built-in analog-to-digital (A/D) converter that produced a digital output signal with 256 gray levels. The three cameras were filtered for spectral observations in the green (555–565 nm), red (625–635 nm), and NIR (845–857 nm) wavelength intervals, respectively. A Cessna 206 aircraft was used to acquire imagery at an

altitude of approximately 1676 m (5500 ft) for field 1 and 2286 m (7500 ft) for field 2 between 1200 and 1400 h local time under sunny conditions. The ground pixel size achieved was approximately 0.67 m for field 1 and 0.92 m for field 2. The images were rectified to the same coordinate system as the QuickBird image based on the ground control points surrounding the fields. For comparison with the QuickBird imagery, the MegaPlus images were resampled to 0.70 m for field 1 and 0.933 m for field 2, which were respectively 1/4 and 1/3 of the cell size (2.8 m) of the QuickBird imagery. For radiometric calibration of the MegaPlus imagery, four 8 m by 8 m tarpaulins with nominal reflectance values of 4, 16, 32 and 48%, respectively, were placed near the fields during image acquisition. The actual reflectance values from the tarpaulins were measured using the FieldSpec spectroradiometer. The rectified multispectral images were converted to reflectance based on three calibration equations (one for each band) relating reflectance values to the digital count values from the four tarps.

Although the two image sets were collected 2 weeks apart when plants were at different growth stages, the correlation between yield and imagery data should have been stable since the imagery were taken shortly after the peak growth of the crop (Yang and Everitt 2002). Based on image data collected from multiple fields and on five dates during the growing season, Yang and Everitt (2002) concluded that images taken about one month after the peak growth provided similar correlations with yield for grain sorghum. This optimal imaging period has important practical implications for image acquisition of this crop. Certainly, it would be ideal if both the airborne and Satellite imagery were acquired on the same day, but because of the scheduling and weather problems 30 May was the first opportunity to acquire the MegaPlus imagery.

A PF3000 grain yield monitor (Ag Leader Technology, Ames, Iowa, USA) integrated with a submeter AgGPS 132 receiver (Trimble Navigation Limited, Sunnyvale, California, USA) was installed on a Case IH 2188 harvester for yield data collection. Instantaneous yield, moisture, and GPS data were simultaneously recorded at one-second intervals. Before grain was harvested from the fields in late June, the yield monitor was calibrated using five calibration loads and an average error of 0.8% and a maximum error of 1.6% were achieved. The yield and GPS data from the yield monitor were viewed and evaluated using SMS Basic software (Ag Leader Technology, Ames, Iowa, USA). Points falling on the top of a harvested path or points with extreme high or low values along each path were first examined and then removed if they were determined to be erroneous. The filtered yield data were exported in ASCII format for further filtering and processing using self-developed programs. An optimum time lag of 15 s as determined using the method by Yang et al. (2002) was used to align yield data with position data. Yield data were adjusted to 14% moisture content.

Since the effective cutting width of the combine was 8.7 m and the average combine speed was approximately 8 km/h or 2.2 m/s, each yield data point represented a rectangular area of 8.7 m by 2.2 m. Evidently the yield data had coarser spatial resolution than either the MegaPlus or QuickBird imagery. In order to match the pixel sizes of the image data, the irregularly-spaced yield data were resampled into regular grids with pixel sizes of 0.70 m for field 1 and 0.933 m for field 2 using the inverse distance to a power and Kriging methods in Surfer (Golden Software, Inc., Golden, Colorado, USA). Two power values of 1 and 2 were applied for the inverse distance method and the linear variogram model was used for Kriging. A search radius of 17 m, approximately twice the cutting width, was used for all the gridding methods. Thus three gridded yield maps or data sets were created for each field.

The QuickBird and MegaPlus images were converted from ERDAS IMAGINE into grids in ArcInfo (ESRI, Inc., Redlands, California, USA). The gridded yield data were also imported from Surfer into ArcInfo. The gridded yield data had the same spatial resolution as the MegaPlus imagery, but had finer resolution than the QuickBird imagery. Therefore, the gridded yield data were aggregated or averaged by a factor of 4 for field 1 and a factor of 3 for field 2 to obtain yield data sets with a cell size of 2.8 m. Yield data sets with a spatial resolution of 8.4 m, which is close to the combine cutting width, were also created. Similarly, new MegaPlus images with pixel sizes of 2.8 m and 8.4 m and new QuickBird images with a pixel size of 8.4 m for the two fields were also generated from their respective high resolution imagery.

Vegetation indices including band ratios and normalized differences (ND) were derived from the individual spectral bands for the images with different resolutions. Band ratios were defined as NB = NIR/Blue, NG = NIR/Green, and NR = NIR/Red; and normalized differences were defined as the blue NDVI or BNDVI = $(\text{NIR} - \text{Blue})/(\text{NIR} + \text{Blue})$, the green NDVI or GNDVI = $(\text{NIR} - \text{Green})/(\text{NIR} + \text{Green})$, and NDVI = $(\text{NIR} - \text{Red})/(\text{NIR} + \text{Red})$. The band ratio, NB, and the normalized difference, BNDVI, only applied to the QuickBird imagery since the MegaPlus imagery did not contain a blue band. Correlation analysis was performed to calculate correlation coefficients (r) between yield and each of the spectral bands and each of the vegetation indices for both types of imagery at different resolutions. Stepwise regression was used to determine the best-fitting equations and their coefficients of determination (R^2) for relating grain yield to the vegetation indices and to the spectral bands for each type of imagery. All the statistical analyses were performed using SAS software (SAS Institute Inc., Cary, North Carolina, USA).

To identify naturally occurring clusters in the image data, the QuickBird imagery was classified into 2 to 5 different categories using an unsupervised classification procedure. Unsupervised classification is the process of sorting out pixels into a finite number of classes using an ISODATA (Iterative Self-Organizing Data Analysis Technique) clustering algorithm. The ISODATA clustering method begins with arbitrary means for a specified number of classes and each pixel is assigned to the closest class based on its spectral distance to each class mean. For the second iteration, the means of all classes are recalculated and the new means are used for the next iteration. The entire process continues until there is little change between iterations. Yield data and spectral data were grouped into respective zones for each of the classifications, and univariate statistics for yield, spectral bands, and vegetation indices were calculated. Multiple comparisons were made among the means for different zones using Fisher's protected least significant difference (LSD) test.

Results and discussion

Figure 1 shows CIR composites of the QuickBird and MegaPlus images for fields 1 and 2. Both the QuickBird and MegaPlus images reveal distinct plant growth patterns within the two fields. Healthy plants showed a reddish-magenta tone while stressed plants and areas with large soil exposure had a bluish and grayish color. The QuickBird imagery was taken at the bloom stage of the plant development (15 May), shortly after the peak growth for the crop. The MegaPlus images were taken 15 days later when the plants were primarily at the soft-dough stage. Despite the difference in plant growth stages, the plants had similar canopy cover during the imaging period. Poor plant canopies in the problem areas within both fields were mainly due to very sandy soil texture. Although pixel sizes are different,

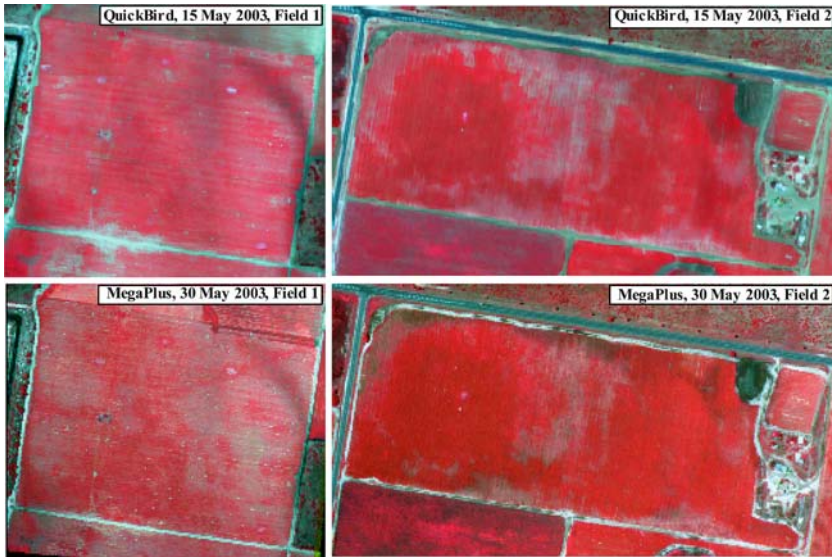


Fig. 1 Color-infrared (CIR) composites of QuickBird and MegaPlus imagery for a 23-ha grain sorghum field (field 1) and a 20-ha grain sorghum field (field 2) in south Texas in 2003

both types of images look fairly similar. However, because of its finer resolution, the MegaPlus image captured more harvester ant beds in field 1 than the QuickBird image. Moreover, the dividing lines on the highway next to field 2 can be visualized on the MegaPlus image, but not on the QuickBird image. These observations indicate that although the QuickBird images could not map small objects that the airborne MegaPlus images could, these high resolution satellite images contain impressive details concerning the crop conditions.

Based on the correlation analysis results, inverse distance to a power of 2 resulted in best correlations between yield and image data. Therefore, the results reported in this paper are based on the yield data created using this gridding method. Tables 1 and 2 summarize the correlation coefficients of grain yield with each spectral band and each vegetation index for both types of imagery at different pixel sizes for fields 1 and 2, respectively. Figure 2 shows the scatter plots and linear regression lines between grain sorghum yield and spectral reflectance for the blue, green, red and NIR bands of QuickBird imagery for field 2. Grain yield was significantly negatively related to the visible bands (blue, green, and red) and positively related to the NIR band and each of the vegetation indices for both fields, though field 2 had higher correlations than field 1 for all the spectral variables. The correlation coefficients tended to increase with pixel size for both the MegaPlus and QuickBird imagery. For the MegaPlus imagery at the original resolutions, the magnitude of the correlation coefficients varied from 0.14 for the NIR band to 0.53 for GNDVI for field 1 and from 0.37 for the NIR band to 0.78 for NG for field 2. For the QuickBird imagery at the 2.8 m resolution, the magnitude of the correlation coefficients varied from 0.26 for the NIR band to 0.59 for the blue band for field 1 and from 0.35 for the NIR band to 0.83 for the blue band, green band or NG for field 2. At the original resolutions, the QuickBird imagery provided better correlations with yield than the MegaPlus imagery. However, because the original yield data had much coarser resolution than the imagery data, the details captured in the imagery, especially in the MegaPlus imagery, could not be found in

Table 1 Correlation coefficients (*r*) between yield monitor data and spectral variables (individual bands and vegetation indices) derived from QuickBird imagery and airborne MegaPlus imagery for a 23-ha grain sorghum field (field 1) in south Texas in 2003

Spectral variable	Pixel = 0.7 m MegaPlus	Pixel = 2.8 m		Pixel = 8.4 m	
		QuickBird	MegaPlus	QuickBird	MegaPlus
Blue	–	–0.59	–	–0.65	–
Green	–0.45 ^a	–0.60	–0.48	–0.64	–0.52
Red	–0.44	–0.56	–0.48	–0.60	–0.52
NIR	0.14	0.26	0.15	0.27	0.16
NB ^b	–	0.56	–	0.63	–
NG	0.52	0.60	0.57	0.66	0.63
NR	0.46	0.55	0.51	0.60	0.56
BNDVI	–	0.54	–	0.60	–
GNDVI	0.53	0.57	0.57	0.63	0.63
NDVI	0.49	0.53	0.53	0.59	0.59

^aAll the *r*-values are significant at the 0.0001 level. The number of pixels used was 472160, 29569, and 3293 for pixel sizes of 0.7, 2.8, and 8.4 m, respectively

^bNB = NIR/Blue, NG = NIR/Green, NR = NIR/Red, BNDVI = (NIR–Blue)/(NIR + Blue), GNDVI = (NIR–Green)/(NIR + Green), and NDVI = (NIR–Red)/(NIR + Red)

Table 2 Correlation coefficients (*r*) between yield monitor data and spectral variables (individual bands and vegetation indices) derived from QuickBird imagery and airborne MegaPlus imagery under different pixel sizes for a 20-ha grain sorghum field (field 2) in south Texas in 2003

Spectral variable	Pixel = 0.933 m MegaPlus	Pixel = 2.8 m		Pixel = 8.4 m	
		QuickBird	MegaPlus	QuickBird	MegaPlus
Blue	–	–0.83	–	–0.88	–
Green	–0.65 ^a	–0.83	–0.67	–0.87	–0.74
Red	–0.60	–0.79	–0.62	–0.84	–0.71
NIR	0.37	0.35	0.39	0.38	0.41
NB ^b	–	0.81	–	0.87	–
NG	0.78	0.83	0.81	0.88	0.85
NR	0.72	0.79	0.75	0.85	0.79
BNDVI	–	0.78	–	0.85	–
GNDVI	0.76	0.81	0.78	0.86	0.83
NDVI	0.69	0.76	0.71	0.83	0.76

^aAll the *r*-values are significant at the 0.0001 level. The number of pixels used was 233700, 26005, and 2888 for pixel sizes of 0.933, 2.8, and 8.4 m, respectively

^bNB = NIR/Blue, NG = NIR/Green, NR = NIR/Red, BNDVI = (NIR–Blue)/(NIR + Blue), GNDVI = (NIR–Green)/(NIR + Green), and NDVI = (NIR–Red)/(NIR + Red)

the gridded yield maps. For example, the true yield for the harvester ant beds or areas with no plant stand in the fields should be zero, but the yield monitor data smoothed out the variability that the imagery detected. As a result, the correlation between yield and image data was reduced. As pixel size approached the actual yield data resolution, the correlation increased. At a pixel size of 8.4 m, the best *r*-values were 0.66 for field 1 and 0.88 for field 2 for the QuickBird imagery, compared with 0.63 for field 1 and 0.85 for field 2 for the MegaPlus imagery. Although the MegaPlus imagery had slightly lower correlations with yield than the QuickBird imagery at 2.8 and 8.4 m resolutions, both types of imagery provided similar results for yield estimation.

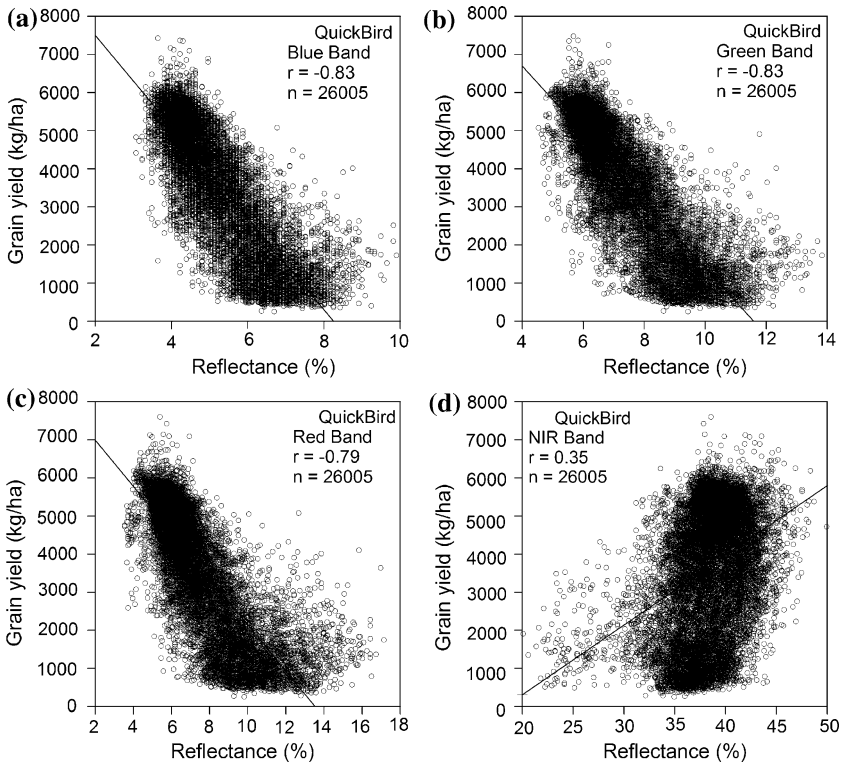


Fig. 2 Scatter plots and linear regression lines between grain sorghum yield and spectral reflectance for the blue, green, red and NIR bands of QuickBird imagery for a 20-ha grain sorghum field (field 2) in south Texas in 2003

Tables 3 and 4 summarize the linear regression results for relating grain yield to the best vegetation indices and the stepwise regression results for relating grain yield to the QuickBird bands and to the MegaPlus bands at different pixel sizes for fields 1 and 2, respectively. For the MegaPlus imagery at the original resolutions, the best vegetation index GNDVI was as good as the three-band combination for field 1 while the best vegetation index NG was better than the three-band combination for field 2. However, the three- and four-band combinations provided better results than the best vegetation indices at the 2.8 m and 8.4 m resolutions for both fields. Similar to the correlation coefficients, the coefficients of determination, R^2 , increased with pixel size for both types of imagery. At the original submeter resolutions, the MegaPlus imagery explained 28% and 61% of the variability in yield for fields 1 and 2, respectively. At 2.8 m resolution, the MegaPlus imagery explained 37% and 67% of the variability for fields 1 and 2, compared with 38% and 71% of the variability accounted for by the three-band QuickBird imagery for the respective fields. With the addition of the blue band in the QuickBird imagery, the R^2 values were only slightly higher. At the 8.4 m resolution, the MegaPlus imagery explained 46% and 77% of the variability in yield for fields 1 and 2, respectively, compared with the three-band QuickBird imagery which explained 49% and 80% of the variability for the respective fields. Although the QuickBird imagery had slightly higher R^2 values than the MegaPlus imagery, both types of imagery accounted for essentially the same amount of

Table 3 Regression results for relating grain yield to the best vegetation indices and to all the spectral bands for airborne MegaPlus imagery and QuickBird imagery at different resolutions for a 23-ha grain sorghum field (field 1) in south Texas in 2003

Pixel size (m)	Image type	Regression equation ^a	Model R ²	SE ^b (kg/ha)
0.7	MegaPlus	Yield = -1755 + 8340*GNDVI ^c	0.28	796
		Yield = 2273 - 335*green + 26*red + 106*NIR	0.28	791
2.8	MegaPlus	Yield = -2537 + 9729*GNDVI	0.33	761
		Yield = 1975 - 873*green + 365*red + 170*NIR	0.37	738
2.8	QuickBird	Yield = -823 + 679*NG	0.36	742
		Yield = 5253 - 866*green + 247*red + 56*NIR	0.38	731
		Yield = 5857 - 389*blue - 743*green + 377*red + 49*NIR	0.39	725
8.4	MegaPlus	Yield = -3608 + 11631*GNDVI	0.40	701
		Yield = 1761 - 1285*green + 605*red + 223*NIR	0.46	665
8.4	QuickBird	Yield = -1476 + 800*NG	0.44	678
		Yield = 5567 - 1551*green + 644*red + 101*NIR	0.49	648
		Yield = 7446 - 1204*blue - 1164*green + 926*red + 79*NIR	0.51	631

^aStepwise regression was used to relate yield to the green, red and NIR bands for both MegaPlus and QuickBird imagery and to all four bands for QuickBird imagery. The best fitting models and all variables in the models were significant at the 0.0001 level. The number of pixels used was 472160, 29569, and 3293 for pixel sizes of 0.7, 2.8, and 8.4 m, respectively

^bSE = Standard error

^cGNDVI = (NIR-Green)/(NIR + Green) and NG = NIR/Green

Table 4 Regression results for relating grain yield to the best vegetation indices and to all the spectral bands for airborne MegaPlus imagery and QuickBird imagery at different resolutions for a 20-ha grain sorghum field (field 2) in south Texas in 2003

Pixel size (m)	Image type	Regression equation ^a	Model R ²	SE ^b (kg/ha)
0.933	MegaPlus	Yield = -2224 + 1345*NG ^c	0.61	1037
		Yield = 2335 - 1179*green + 436*red + 235*NIR	0.57	1088
2.8	MegaPlus	Yield = -2635 + 1442*NG	0.66	962
		Yield = 1686 - 1947*green + 1022*red + 315*NIR	0.67	946
2.8	QuickBird	Yield = -2555 + 1151*NG	0.69	919
		Yield = 7480 - 1444*green + 865*red + 90*NIR	0.71	880
		Yield = 8198 - 550*blue - 1141*green + 523*red + 75*NIR	0.72	869
8.4	MegaPlus	Yield = -3042 + 1539*NG	0.72	861
		Yield = 1522 - 2453*green + 1371*red + 366*NIR	0.77	776
8.4	QuickBird	Yield = -3187 + 1272*NG	0.78	771
		Yield = 6934 - 2026*green + 870*red + 138*NIR	0.80	723
		Yield = 7963 - 725*blue - 1526*green + 872*red + 112*NIR	0.81	719

^aStepwise regression was used to relate yield to the green, red and NIR bands for both MegaPlus and QuickBird imagery and to all four bands for QuickBird imagery. The best fitting models and all variables in the models were significant at the 0.0001 level. The number of pixels used was 233700, 26005, and 2888 for pixel sizes of 0.933, 2.8, and 8.4 m, respectively

^bSE = Standard error

^cNG = NIR/Green

yield variability, indicating that the QuickBird imagery was as effective as the MegaPlus imagery for yield estimation at the 2.8 m and 8.4 m resolutions. As discussed previously, because of the coarser resolution of the yield data, the correlation coefficients between yield and the imagery were underestimated at the finer imagery resolutions. As pixel size

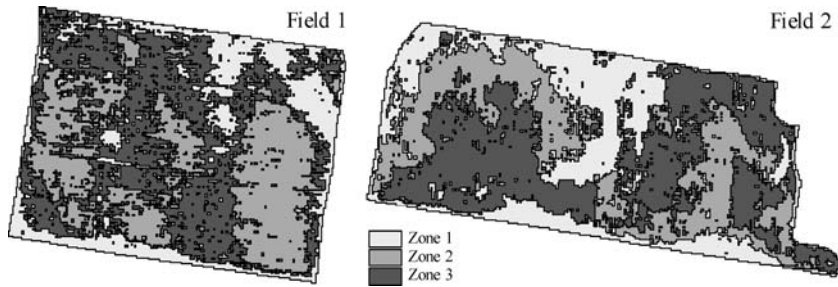


Fig. 3 Three-zone unsupervised classification maps of QuickBird imagery for two grain sorghum fields in south Texas in 2003. Zones 1, 2, and 3 represent low, medium, and high production areas, respectively, within the fields

increased toward the yield data resolution, the image data were smoothed and the correlations improved.

Figure 3 shows the three-zone unsupervised classification maps of the QuickBird imagery for fields 1 and 2. Zones 1, 2, and 3 represent low, medium, and high production areas, respectively. Since these classification maps were not filtered, the small inclusions of other classes exist within the dominant class. These classification maps clearly reveal plant growth and yield patterns within the fields.

Tables 5 and 6 summarize means and standard deviations of grain yield and reflectance for the four spectral bands for the whole field and individual zones for the two-, three-, four-, and five-zone classifications for fields 1 and 2, respectively. Field 1 had a mean yield of 2937 kg/ha with a standard deviation of 927 kg/ha while field 2 had a higher mean yield of 3679 kg/ha with a larger standard deviation of 1655 kg/ha. The coefficient of variation was 32% for field 1 and 45% for field 2. Clearly the spatial variability in yield was larger in

Table 5 Means and standard deviations of grain yield and reflectance for four spectral bands for the whole field and each of its zones for two-, three-, four-, and five-zone classifications based on 2.8-m QuickBird imagery for a 23-ha grain sorghum field (field 1) in south Texas in 2003

Field/zone	Area (ha)	No. of Samples	Yield		Blue		Green		Red		NIR	
			Mean (kg/ha)	STD ^a (kg/ha)	Mean (%)	STD (%)	Mean (%)	STD (%)	Mean (%)	STD (%)	Mean (%)	STD (%)
Whole	23.25	29569	2937	927	4.9	0.8	7.4	1.1	7.4	1.7	40.0	3.1
Zone 1	5.02	6352	2309 ^{a,b}	949	5.5 ^a	1.2	8.0 ^a	1.7	8.7 ^a	2.9	35.4 ^a	3.0
Zone 2	18.23	23217	3109 ^b	843	4.8 ^b	0.5	7.2 ^b	0.7	7.0 ^b	1.0	41.1 ^b	1.7
Zone 1	5.19	6568	2327 ^a	950	5.5 ^a	1.2	8.0 ^a	1.7	8.7 ^a	2.9	35.5 ^a	3.0
Zone 2	8.49	10826	2961 ^b	789	4.8 ^b	0.5	7.4 ^b	0.7	7.1 ^b	0.9	42.7 ^c	1.0
Zone 3	9.57	12175	3245 ^c	867	4.7 ^c	0.5	7.0 ^c	0.7	6.9 ^c	1.0	40.0 ^b	0.9
Zone 1	2.07	2607	1743 ^a	906	6.7 ^a	1.2	9.6 ^a	1.6	11.4 ^a	2.7	35.1 ^a	4.4
Zone 2	3.34	4243	2683 ^b	781	4.8 ^b	0.5	7.0 ^d	0.7	6.9 ^c	1.0	36.1 ^b	1.8
Zone 3	8.41	10722	2959 ^c	786	4.8 ^b	0.5	7.4 ^b	0.7	7.1 ^b	0.9	42.7 ^d	1.0
Zone 4	9.43	11997	3267 ^d	855	4.7 ^d	0.4	7.0 ^d	0.6	6.8 ^d	0.9	40.0 ^c	0.9
Zone 1	1.42	1782	1556 ^a	929	7.1 ^a	1.2	10.1 ^a	1.6	12.4 ^a	2.7	33.7 ^a	4.4
Zone 2	4.90	6233	2518 ^b	716	5.2 ^b	0.5	7.7 ^b	0.8	7.9 ^b	1.1	38.9 ^c	3.2
Zone 3	4.62	5865	2832 ^c	815	4.8 ^c	0.5	7.1 ^d	0.6	7.1 ^c	0.9	38.0 ^b	0.9
Zone 4	5.23	6675	2951 ^d	717	4.8 ^c	0.4	7.3 ^c	0.6	7.0 ^d	0.8	43.2 ^c	0.9
Zone 5	7.08	9014	3558 ^c	769	4.5 ^c	0.3	6.7 ^c	0.4	6.4 ^c	0.6	40.8 ^d	0.8

^aSE = Standard error

^bMeans for each classification within a column followed by the same letter are not significantly different at the 0.0001 probability level, according to Fisher's least significant difference test

Table 6 Means and standard deviations of grain yield and reflectance for four spectral bands for the whole field and each of its zones for two-, three-, four-, and five-zone classifications based on 2.8-m QuickBird imagery for a 20-ha grain sorghum field (field 2) in south Texas in 2003

Field/zone	Area (ha)	No. of Samples	Yield		Blue		Green		Red		NIR	
			Mean (kg/ha)	STD ^a (kg/ha)	Mean (%)	STD (%)	Mean (%)	STD (%)	Mean (%)	STD (%)	Mean (%)	STD (%)
Whole	20.39	26005	3679	1655	5.2	1.1	7.4	1.6	7.5	2.2	38.4	3.1
Zone 1	6.08	7754	1897 ^{a,b}	1108	6.6 ^a	0.9	9.2 ^a	1.3	10.0 ^a	2.0	35.6 ^a	3.2
Zone 2	14.31	18251	4436 ^b	1208	4.6 ^b	0.6	6.7 ^b	0.9	6.4 ^b	1.0	39.6 ^b	2.2
Zone 1	5.95	7586	1747 ^a	980	6.7 ^a	0.8	9.4 ^a	1.1	10.2 ^a	1.7	36.0 ^a	3.4
Zone 2	6.36	8110	4206 ^b	1241	4.7 ^b	0.6	6.9 ^b	0.9	6.5 ^b	1.0	41.5 ^c	1.5
Zone 3	8.08	10309	4686 ^c	1007	4.5 ^c	0.5	6.4 ^c	0.7	6.2 ^c	0.8	37.7 ^b	1.5
Zone 1	3.81	4859	1641 ^a	916	6.9 ^a	0.8	9.6 ^a	1.2	10.7 ^a	1.9	34.5 ^a	3.3
Zone 2	3.35	4275	2253 ^b	1165	6.1 ^b	0.6	8.8 ^b	0.9	9.0 ^b	1.2	39.2 ^c	1.3
Zone 3	5.45	6956	4466 ^c	1065	4.6 ^c	0.5	6.6 ^c	0.7	6.2 ^c	0.8	41.7 ^d	1.5
Zone 4	7.77	9915	4740 ^d	958	4.4 ^d	0.5	6.3 ^d	0.6	6.1 ^d	0.8	37.7 ^b	1.5
Zone 1	2.96	3778	1400 ^a	730	7.2 ^a	0.7	10.1 ^a	1.0	11.4 ^a	1.6	34.8 ^a	3.8
Zone 2	3.28	4188	2303 ^b	1184	6.0 ^b	0.5	8.6 ^b	0.7	8.8 ^b	1.0	39.2 ^d	1.3
Zone 3	2.55	3257	3257 ^c	1235	5.2 ^c	0.7	7.3 ^c	0.9	7.4 ^c	1.1	34.9 ^b	1.5
Zone 4	4.32	5512	4362 ^d	1095	4.6 ^d	0.5	6.7 ^d	0.7	6.2 ^d	0.8	42.1 ^c	1.4
Zone 5	7.27	9270	4971 ^e	776	4.3 ^c	0.4	6.2 ^c	0.5	6.0 ^c	0.7	38.6 ^c	1.0

^aSE = Standard error^bMeans for each classification within a column followed by the same letter are not significantly different at the 0.0001 probability level, according to Fisher's least significant difference test

field 2 than in field 1. Grain yield differed significantly among the respective zones for each of the four classifications in fields 1 and 2. Mean reflectance values for the four spectral bands differed significantly among the respective zones for each of the four classifications in both fields, except that no significant differences in blue reflectance were found between two of the zones for the four- and five-zone classifications for field 1. Mean yield was inversely related to means for the blue, green, and red bands for each of the four classifications in both fields. Although mean yield was generally positively related to the means for the NIR band, the associations between the means for yield and the means for the NIR band were mixed among the zones for some of the classifications. These results agree with those from the correlation analyses.

Conclusions

The high spatial resolution QuickBird satellite imagery used in this study clearly revealed plant growth variability and was significantly related with grain yield monitor data. Moreover, the QuickBird imagery at its original 2.8 m resolution had better correlations with yield than the MegaPlus imagery at its submeter resolution, but both types of imagery provided similar correlations with yield as image pixel size approached yield data resolution. These results indicate that QuickBird imagery can be a useful data source for mapping within-field crop growth and yield variability. The procedures illustrated in this article can be used for integrating QuickBird imagery with airborne imagery and yield monitor data for mapping crop yield.

Acknowledgements We thank Rene Davis and Fred Gomez for acquiring the MegaPlus imagery for this study and Jim Forward for assistance in image rectification. Thanks are also extended to Bruce Campbell and Rio Farms, Inc. at Monte Alto, TX, for use of their fields and harvest equipment.

References

- Barnes EM, Baker MG (2000) Multispectral data for mapping soil texture: possibilities and limitations. *Appl Eng Agric* 16(6):731–741
- Escobar DE, Everitt JH, Noriega JR, Davis MR, Cavazos I (1997) A true digital imaging system for remote sensing applications. In: Everitt JH, (ed.) Proceedings of 16th biennial workshop on color photography and videography in resource assessment. Bethesda, Maryland, USA, American Society for Photogrammetry and Remote Sensing, pp 470–484
- Escobar DE, Everitt JH, Noriega JR, Cavazos I, Davis MR (1998) A twelve-band airborne digital video imaging system (ADVIS). *Remote Sens Environ* 66:122–128
- Everitt JH, Escobar DE, Cavazos I, Noriega JR, Davis MR (1995) A three-camera multispectral digital video imaging system. *Remote Sens Environ* 54:333–337
- Gopal Pillai S, Tian L (1999) In-field variability detection and spatial yield modeling for corn using digital aerial imaging. *Transact ASAE* 42(6):1911–1920
- Johannsen CJ, Carter PG, Willis PR, Owubah E, Erikson B, Ross K, Targulian N (1998) Applying remote sensing technology to precision farming. In: Roberts PC, Rust RH, Larson WE (eds) Proceedings of 4th international conference on precision agriculture. Madison, Wisconsin, USA, ASA/CSSA/SSSA, pp 1413–1422
- Mao C, Kettler D (1995) Digital CCD cameras for airborne remote sensing. In: Mausel PW (ed.) Proceedings of 15th biennial workshop on color photography and videography in resource assessment. Bethesda, Maryland, USA, American Society for Photogrammetry and Remote Sensing, pp 1–12
- Pinter PJ, Jr, Hatfield JL, Schepers JS, Barnes EM, Moran MS, Daughtry CST, Upchurch DR (2003) Remote sensing for crop management. *Photogram Eng Remote Sens* 69(6):647–664
- Robert PC (1996) Use of remote sensing imagery for precision farming. In: Proceedings of 26th international symposium on remote sensing of environment and 18th symposium of the canadian remote sensing society, Vancouver, BC, Canada, International Symposia on Remote Sensing of Environment and Symposia of the Canadian Remote Sensing Society, pp 596–599
- Senay GB, Ward AD, Lyon JG, Fausey NR, Nokes SE (1998) Manipulation of high spatial resolution aircraft remote sensing data for use in site-specific farming. *Transact ASAE* 41(2):489–495
- Shanahan JF, Schepers JS, Francis DD, Varvel GE, Wilhelm WW, Tringe JM, Schlemmer MR, Major DJ (2001) Use of remote sensing imagery to estimate corn grain yield. *Agron J* 93:583–589
- Thenkabail PS, Ward AD, Lyon JG (1995) Landsat-5 Thematic Mapper models of soybean and corn crop characteristics. *Int J Remote Sens* 15:49–61
- Tucker CJ, Holben BN, Elgin JH Jr (1980) Relationship of spectral data to grain yield variation. *Photogram Eng Remote Sens* 46(5):657–666
- Wiegand CL, Richardson AJ (1990) Use of spectral vegetation indices to infer leaf area, evapotranspiration and yield: I. Rationale. *Agron J* 82(3):623–629
- Yang C, Everitt JH, Bradford JM, Escobar DE (2000) Mapping grain sorghum growth and yield variations using airborne multispectral digital imagery. *Transact ASAE* 43(6):1927–1938
- Yang C, Everitt JH, Bradford JM (2002) Optimum time lag determination for yield monitoring with remotely sensed imagery. *Transact ASAE* 45(6):1737–1745
- Yang C, Anderson GL (1999) Airborne videography to identify spatial plant growth variability for grain sorghum. *Precis Agric* 1(1):67–79
- Yang C, Everitt JH (2002) Relationships between yield monitor data and airborne multitemporal multispectral digital imagery for grain sorghum. *Precis Agric* 3(4):373–388